Impedance Spectroscopy Characterization of Highly Attenuating Piezocomposites

Andrey RYBIANETS, Yoram ESHEL, Ultrashape Ltd., Tel-Aviv, Israel
Ron TASKER, TASI Technical Software Inc., Kingston, Ontario, Canada

Abstract. This paper presents the results of a comparative experimental investigation of proprietary polymer-free polycrystalline composites (porous ceramics, piezocomposites ceramics/crystals) developed and manufactured by Ultrashape Ltd. Both the IEEE Standards and ultrasonic methods together with the Piezoelectric Resonance Analysis Program (PRAP) were used to determine material constants. The PRAP software (TASI Technical Software Inc.) enables complete automatic analysis of resonance impedance spectra by comparing the predicted dependence of impedance on frequency with an impedance spectrum measured on a sample of appropriate geometry and dimensions to derive complex elastic, dielectric, and piezoelectric properties of the resonator. Material constants obtained by the different methods were compared. The results show that the impedance spectroscopy method gives more precise data and in some cases is the "sheet anchor" of correct values for materials with extremely low Q.

1. Introduction

Demands on medical and NDT ultrasonic transducer performance have increased in recent years. Low-Q piezoceramics and piezocomposite materials are widely used for wide-band NDT ultrasonic transducers with high sensitivity and resolution. Some of these advanced materials are lossy and direct use of IEEE Standards for material constant determination leads to significant errors. The modeling and design of piezoelectric devices by finite element methods, among others, relies on the accuracy of the dielectric, piezoelectric and elastic coefficients of the active material used; commonly an anisotropic ferroelectric polycrystal. The accurate description of piezoceramics must include the evaluation of the dielectric, piezoelectric and mechanical losses, accounting for the out-of-phase material response to the input signal.

The basic techniques for finding material constants of piezoelectric materials are outlined in the IEEE Standard on Piezoelectricity (1987) [1]. These methods work for many of the most widely used commercial piezoceramics based on lead-titanate-zirconate (PZT) compositions that are high-Q_M and high-coupling coefficient piezoelectric materials. However, there is a general agreement that their use in many new piezoelectric materials such as porous ceramics, piezoelectric polymers or piezoelectric composites may lead to significant errors. Furthermore, the current IEEE Standard does not comprehensively account for the complex nature of material coefficients, using only the dielectric loss factor ($\tan \delta$) and the mechanical quality factor (Q_M) to account for loss.

Numerous techniques using complex material constants have been proposed to take into account losses in low-Q_M materials and to overcome limitations in the IEEE Standard [2-6]. Iterative methods [7-9] provide the way to accurately determine the complex

coefficients in the linear range of poled piezoceramics from complex impedance resonance measurements. The PRAP automatic iterative method [10] has been applied in this work to the full set of standard geometries and resonance modes needed to complete complex characterization in a wide range of materials with very high and moderate loss factors.

2. Piezoelectric Resonance Analysis Methods

In the direct piezoelectric effect charge is generated from applying a stress to a specimen. In the converse piezoelectric effect, the specimen will undergo strain in response to an electric field. By consideration of four possible thermodynamic potentials in the case of adiabatic, isothermal and low amplitude conditions [11,12], the linear equations of piezoelectricity give the relationship between electric field (E), dielectric displacement (D), strain (S) and stress (T):

$$S_p = s^D_{pq} T_q + g_{pm} D_m \qquad (1)$$

$$E_m = \beta^T_{mn} D_n - g_{pm} T_p$$

$$S_p = s^E_{pq} T_q + d_{pm} E_m \qquad (2)$$

$$D_m = \varepsilon^T_{mn} E_n + d_{pm} T_p$$

$$T_p = c^E_{pq} S_q - e_{pm} E_m \qquad (3)$$

$$D_m = \varepsilon^S_{mn} E_n + e_{pm} S_p$$

$$T_p = c^D_{pq} S_q - h_{pm} D_m \qquad (4)$$

$$E_m = \beta^S_{mn} D_n - h_{pm} S_p$$

In equations (1-4) d, e, g, and h are the piezoelectric constants, s and c are the elastic compliance and stiffness at constant E and D, and ε and β are the permittivity and inverse permittivity at constant S and T. The mechanical variables have three additional shear directions (4, 5, 6) while the electrical variables are only in the three standard directions (1, 2, 3).

Each of the above sets of equations is typically represented as the piezoelectric matrix with the transpose of the piezoelectric constants in the top right corner. Symmetry in materials means that many of the elements of the piezoelectric matrix are either equal, zero, or some function of themselves. Poled polycrystalline materials are of the C_∞ or 6mm symmetry, and similar to the other sets of equations, equation set (2) reduces to a form of the piezoelectric matrix that includes only 10 independent constants:

$$\begin{bmatrix} S_1 \\ S_2 \\ S_3 \\ S_4 \\ S_5 \\ S_6 \\ D_1 \\ D_2 \\ D_3 \end{bmatrix} = \begin{bmatrix} s^E_{11} & s^E_{12} & s^E_{13} & 0 & 0 & 0 & 0 & 0 & d_{31} \\ s^E_{12} & s^E_{11} & s^E_{13} & 0 & 0 & 0 & 0 & 0 & d_{31} \\ s^E_{13} & s^E_{13} & s^E_{33} & 0 & 0 & 0 & 0 & 0 & d_{33} \\ 0 & 0 & 0 & s^E_{55} & 0 & 0 & 0 & d_{15} & 0 \\ 0 & 0 & 0 & 0 & s^E_{55} & 0 & d_{15} & 0 & 0 \\ 0 & 0 & 0 & 0 & 0 & 2\left(s^E_{11} - s^E_{12}\right) & 0 & 0 & 0 \\ 0 & 0 & 0 & 0 & d_{15} & 0 & \varepsilon^T_{11} & 0 & 0 \\ 0 & 0 & 0 & d_{15} & 0 & 0 & 0 & \varepsilon^T_{11} & 0 \\ d_{31} & d_{31} & d_{33} & 0 & 0 & 0 & 0 & 0 & \varepsilon^T_{33} \end{bmatrix} \begin{bmatrix} T_1 \\ T_2 \\ T_3 \\ T_4 \\ T_5 \\ T_6 \\ E_1 \\ E_2 \\ E_3 \end{bmatrix} \qquad (5)$$

In general the material constants are temperature (relative to the Curie temperature for ferroelectrics), time (logarithmic relaxation since poling) and frequency dependant. In reality the properties may also be field-dependant which would require a re-derivation of the piezoelectric equations for higher order field terms.

Impedance spectroscopy characterization stems from the relation for impedance Z:

$$\mathbf{Z} = V/\mathbf{I} = \int \mathbf{E} \cdot d\mathbf{x} \Big/ A\frac{d\mathbf{D}}{dt}, \qquad (6)$$

where V is voltage, I is current, and A is the surface area over which current is measured. The piezoelectric equations give the relationship between D and E through stress and strain. For simple 1-dimensional resonance modes, many of the electric and mechanical field variables go to zero and the sets of piezoelectric equations decouple.

Solving the wave equation for one-dimensional steady-state displacement in the specimen and evaluating S from the derivative of displacement, together with the boundary conditions of an unclamped resonator, the piezoelectric equations can be used to evaluate the relationship between D and E as a function of frequency and material properties. The impedance of a thickness extensional (TE) resonator reduces to [13]:

$$\mathbf{Z} = \frac{\boldsymbol{\beta}_{33}^{S} l + \dfrac{\mathbf{h}_{33}^{2}}{\sqrt{\rho \mathbf{c}_{33}^{D}}\,\omega} \tan\left(\dfrac{\omega l \sqrt{\rho}}{2\sqrt{\mathbf{c}_{33}^{D}}}\right)}{i\omega A}, \qquad (7)$$

where ρ is specimen density, ω is angular frequency and l is thickness of the sample in the direction of poling. For the TE resonator the lateral dimensions must be at least 10 times the thickness to assure a clean 1-dimensional TE mode. This can be relaxed slightly in low Q materials. In impedance spectroscopy characterization of piezoelectrics the material properties of equation (7) can be adjusted until the impedance fits a measured impedance spectrum as a function of frequency.

The common one-dimensional 6mm modes include the Length Extensional (LE), Thickness Extensional (TE), Length-Thickness Extensional (LTE), Thickness Shear (TS), Length Shear (LS), and Radial modes. Each of these modes provides electrical, elastic and piezoelectric properties of the material. Table 1 lists the properties of one form of the reduced piezoelectric matrix with the modes that will provide those properties.

Table 1. ***Properties Provided by the Common Modes***

Property	ε^{T}_{11}	ε^{T}_{33}	s^{E}_{11}	s^{E}_{12}	s^{E}_{13}	s^{E}_{33}	s^{E}_{55}	d_{13}	d_{33}	d_{15}
Mode	*TS, LS*	*LE, LTE, Radial*	*LTE, Radial*	*Radial*		*LE*	*LS, TS*	*LTE, Radial*	*LE*	*TS, LS*

By analyzing specimens inducing the TS, LE and Radial modes, all but s^{E}_{13} of the reduced 6mm piezoelectric matrix can be obtained. s^{E}_{13} can be found from the properties determined with the TE, LTE and LE modes for other representations of the piezoelectric linear equations [8] meaning all modes but the LS mode are required to construct the piezoelectric matrix. Alternatively, using an initial guess for s^{E}_{13} the reduced matrix can be inverted and c^{D}_{13} compared that found for the TE mode, eliminating need for the LTE mode.

In practice, material properties are dispersive (vary with frequency). This means that the range of frequency used to fit forms of equation (6) to measured spectra should be limited. It is worth noting that only a few points in the spectrum are required to determine properties. For the TE mode, only three points are required.

The IEEE Standard on Piezoelectricty (1987) [1] describes two approaches to obtaining material properties using either the difference between parallel (f_p) and series (f_s) resonance frequencies, or the frequency ratio between different order resonance peaks. This

can be problematic when material properties are dispersive or when a low electromechanical coupling constant results in a small difference between f_p and f_s.

Smits [8] proposed a general method for the TE, TS, LE and LTE resonators using three points around resonance. This method does not rely on critical frequencies in the spectrum and so does not lose sensitivity for low Q materials. At resonance and anti-resonance, currents can be very large and small and this presents an instrumentation problem. Though less an issue for low Q materials, Smits' method is less demanding of instrumentation than the IEEE methods. Finally, because the choice of analysis points is somewhat arbitrary, noisy spectra and samples with mode coupling may still be analyzed using Smits' method. The IEEE Standard in Piezoelectricity (1987) treats all material properties as real, evaluating mechanical and electrical loss independently through Q_M and tanδ. Losses in the electromechanical coupling constant were assumed zero. This was acceptable for low loss piezoelectric materials such as PZT, but can lead to significant errors when materials have large loss. In real materials the complex impedance results from complex material properties [3]. This is directly associated with dielectric conduction losses [14] and attenuation of the displacement wave in the sample.

The Piezoelectric Resonance Analysis Program [10] analyses impedance spectra to determine complex material properties. This software uses a generalized form of Smits' method to determine material properties for any common resonance mode, and a generalized ratio method for the radial mode [15] valid for all material Q's. By analyzing on each harmonic, complex material properties as a function of frequency can be determined. The software always generates an impedance spectrum from the determined properties to indicate validity of the results.

3. Experimental Results and Discussion

The extremely low-Q piezoceramic composites A850L-20 and moderately low-Q porous ceramics U1-20S manufactured by Ultrashape Ltd. were chosen for comparison between the IEEE Standard and PRAP methods of resonance measurements. Complex electrical coefficients of piezocomposite elements were determined by impedance spectroscopy method using Piezoelectric Resonance Analysis (PRAP) software [10].

Measurements were made using the Solartron Impedance/Gain-Phase Analyzer SL 1260. Sound velocity and attenuation of longitudinal waves in composite samples were measured by pulse–echo and through-transmit ultrasonic methods in the frequency range 1-5 MHz using a LeCroy Wave Surfer 422 digital oscilloscope and Olympus 5800 and 5077 pulser/receivers using standard Olympus transducers.

Figure 1 and 2 show impedance spectra and PRAP approximations for thickness and radial modes of A850L-20 piezoceramic composite disks (Ø20x 0.8 mm). Complex constants of A850L-20 disk (Ø20 x 0.8 mm), obtained using PRAP analysis for thickness and radial resonance modes as well as corresponding IEEE Standard results are summered in Tables 1 and 2. Additional physical parameters of A850L-20 composite measured by ultrasonic method are as follows: Z_A = 22.8 MRayl, ρ = 6.4 g/cm3, V_t = 3568 m/c., Q_M = 3.

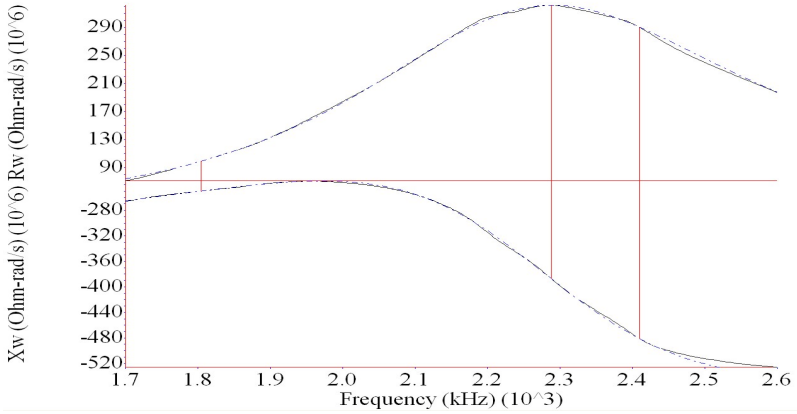

Figure 1. Impedance spectra and PRAP approximations for TE mode of A850L-20 disk.

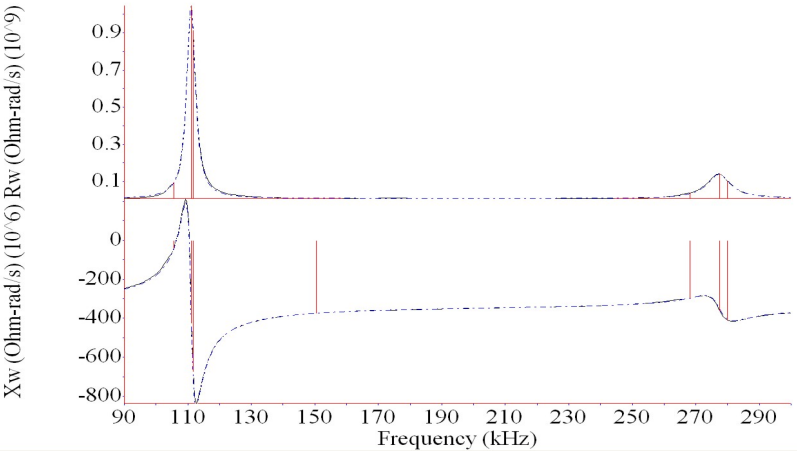

Figure 2. Impedance spectra and PRAP approximations for radial extensional mode of A850L-20 disk.

It can be seen from Tables 1 and 2 that the discrepancy between PRAP and IEEE Standard results for very low-Q ceramic composites were greater than 5%. The new ceramic piezocomposite A850L-20 manufactured by Ultrashape Ltd. is characterized by previously unachievable low Q (Q^t_M=3) combined with high piezoelectric (d33=300) and electromechanical (k_t = 0.5) parameters, high Curie point (340°C) and low acoustic impedance (22 MRayl) in a wide working frequency range (0.2-12 MHz). For lower k samples even greater differences would be expected.

Table 1. PRAP Analysis Results for TE Mode of A850L-20 disk

PRAP Parameter	**Real**	**Imaginary**	**IEEE Standard**	**%Error**
f_p *(Hz)*	$2.26 \cdot 10^6$	*340289*	$2.29 \cdot 10^6$	*1.3*
f_s *(Hz)*	$2.01 \cdot 10^6$	*304601*	$2.01 \cdot 10^6$	*0.0*
k_t	*0.492734*	*-0.00138*	*0.513653*	*4.3*
c_{33}^D *(N/m²)*	$8.15 \cdot 10^{10}$	$2.52 \cdot 10^{10}$	$8.58 \cdot 10^{10}$	*5.3*
c_{33}^E *(N/m²)*	$6.17 \cdot 10^{10}$	$1.92 \cdot 10^{10}$	$6.31 \cdot 10^{10}$	*2.3*
e_{33} *(C/m²)*	*10.6185*	*1.31335*	-	
h_{33} *(V/m)*	$1.91 \cdot 10^9$	$3.29 \cdot 10^8$	-	
ε_{33}^S *(F/m)*	$5.52 \cdot 10^{-9}$	$-2.64 \cdot 10^{-10}$	-	

Table 2. PRAP Analysis Results for Radial Extensional Mode A850L-20 disk

PRAP Parameter	Real	Imaginary	IEEE Standard	%Error
f_s1 (Hz)	105834	1737.27	106037	0.2
f_p1 (Hz)	110947	1623.38	111192	0.2
f_s2 (Hz)	275536	4522.35	275194	0.1
S_{11}^E (m²/N)	$1.72 \cdot 10^{-11}$	$-5.66 \cdot 10^{-13}$	$1.75 \cdot 10^{-11}$	1.7
S_{12}^E (m²/N)	$-5.84 \cdot 10^{-12}$	$1.92 \cdot 10^{-13}$	$-6.14 \cdot 10^{-12}$	5.1
$-d_{31}$ (C/N)	$7.35 \cdot 10^{-11}$	$-3.59 \cdot 10^{-12}$	$7.38 \cdot 10^{-11}$	0.4
ε_{33}^T (F/m)	$8.27 \cdot 10^{-9}$	$-2.38 \cdot 10^{-10}$	$8.29 \cdot 10^{-9}$	0.2
k_p	0.339052	-0.00613	0.340468	0.4
σ^P	0.339174	$8.34 \cdot 10^{-6}$	0.351532	3.6
e_{31} (C/m²)	6.46184	-0.10351	6.51219	0.8
S_{66}^E (m²/N)	$4.61 \cdot 10^{-11}$	$-1.51 \cdot 10^{-12}$	$4.72 \cdot 10^{-11}$	2.4
C_{66}^E (N/m²)	$2.16 \cdot 10^{10}$	$7.10 \cdot 10^{8}$	$2.12 \cdot 10^{10}$	1.9

Figure 3 shows impedance spectra and PRAP approximations for the TE mode of a U1-20 porous ceramic disk (Ø10x 0.5 mm). Complex constants for a U1-20 disk (Ø10 x 0.5 mm) with moderately low Q obtained using PRAP analysis for thickness and radial resonance modes as well as corresponding IEEE Standard results are summered in Tables 3 and 4. Additional physical parameters of U1-20 porous ceramics measured by the ultrasonic method for a disc are as follows: Z_A = 25.5 Mrayl, ρ = 6.6 g/cm3, V_t = 3875 m/c., Q_M = 25.

It is readily observed in Tables 3 and 4 that for moderately low-Q ceramic composites the results obtained by PRAP and the IEEE Standard methods are similar. However, even in this case PRAP gives sets of complex constants, allowing thereby account and analysis of the losses. Porous ceramics U1-20 manufactured by Ultrashape Ltd. is characterized by the moderate low Q^t_M = 30, high electromechanical coupling factor k_t = 0.57, low acoustic impedance (25 MRayl) and are used for medical and NDT ultrasonic transducers design.

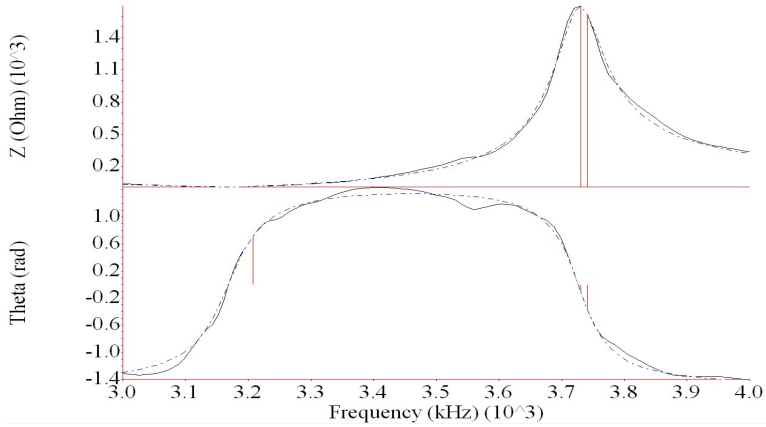

Figure 3. Impedance spectra and PRAP approximations for TE mode of U1-20 disk.

PRAP was used to determine material properties from higher order harmonics, and the results are illustrated in Figures 4 and 5. Figure 4 shows the impedance spectrum and PRAP approximation for the second order peak (3 natural harmonic) of the TE mode of a U1-20 porous ceramic disk.

Table 3. PRAP Analysis Results for TE Mode of U1-20S disk

PRAP Parameter	Real	Imaginary	IEEE Standard	%Error
f_p (Hz)	$3.73 \cdot 10^6$	37771.9	$3.73 \cdot 10^6$	0.0
f_s (Hz)	$3.17 \cdot 10^6$	44838.1	$3.17 \cdot 10^6$	0.0
k_t	0.566103	-0.00555	0.56646	0.1
c_{33}^D (N/m²)	$9.91 \cdot 10^{10}$	$2.01 \cdot 10^9$	$9.93 \cdot 10^{10}$	0.2
c_{33}^E (N/m²)	$6.74 \cdot 10^{10}$	$1.99 \cdot 10^9$	$6.75 \cdot 10^{10}$	0.2
e_{33} (C/m²)	8.3419	-0.25107	-	
h_{33} (V/m)	$3.81 \cdot 10^9$	$1.17 \cdot 10^8$	-	
ε_{33}^S (F/m)	$2.19 \cdot 10^{-9}$	$-1.33 \cdot 10^{-10}$	-	

Table 4. PRAP Analysis Results for Radial Extensional Mode U1-20S disk

PRAP Parameter	Real	Imaginary	IEEE Standard	%Error
f_s1 (Hz)	201059	1743.34	200820	0.1
f_p1 (Hz)	222222	754.256	221340	0.4
f_s2 (Hz)	531110	3166.76	531294	0.0
s_{11}^E (m²/N)	$1.75 \cdot 10^{-11}$	$-8.91 \cdot 10^{-14}$	$1.74 \cdot 10^{-11}$	0.6
s_{12}^E (m²/N)	$-4.99 \cdot 10^{-12}$	$1.48 \cdot 10^{-13}$	$-4.87 \cdot 10^{-12}$	2.4
$-d_{31}$ (C/N)	$7.92 \cdot 10^{-11}$	$-4.36 \cdot 10^{-12}$	$7.76 \cdot 10^{-11}$	2.0
ε_{33}^T (F/m)	$4.35 \cdot 10^{-9}$	$-1.97 \cdot 10^{-10}$	$4.27 \cdot 10^{-9}$	1.8
k_p	0.479629	-0.01101	0.47302	1.4
σ^P	0.284483	0.009907	0.278866	2.0
e_{31} (C/m²)	6.32055	-0.22792	6.16393	2.5
s_{66}^E (m²/N)	$4.5 \cdot 10^{-11}$	$1.18 \cdot 10^{-13}$	$4.46 \cdot 10^{-11}$	0.9
c_{66}^E (N/m²)	$2.22 \cdot 10^{10}$	5.841 ·107	$2.24 \cdot 10^{10}$	0.9

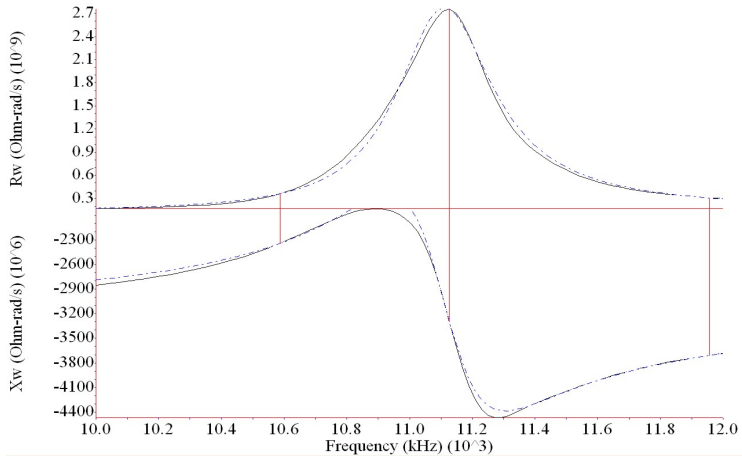

Figure 4. Impedance spectra and PRAP approximations for second order peak (3 natural harmonic) of TE mode of U1-20 porous ceramic disk

Figure 5 shows results from PRAP for complex c^D_{33} obtained from the harmonics of the TE mode of a U1-20 porous ceramic disk. It is readily observed that c^D_{33} (real) decrease and c^D_{33} (imaginary) increase significantly with the frequency. Therefore mechanical quality factor Q_M decreases significantly as a result of Rayleigh scattering of high frequency ultrasonic

waves on pores. This also indicates the importance of stating frequency with tabulated material properties.

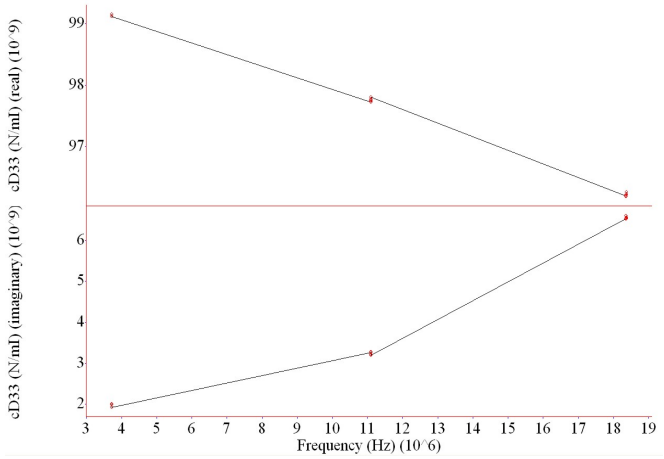

Figure 5. Frequency dependence of c^{D}_{33} (real) and c^{D}_{33} (imaginary) obtained by PRAP for higher orders peaks of TE mode of a U1-20 porous ceramic disk.

4. Summary

A comparative experimental investigation of proprietary polycrystalline composites with very low and moderate Q_M developed and manufactured by Ultrashape Ltd was presented. The IEEE Standard on piezoelectricity and ultrasonic methods together with the Piezoelectric Resonance Analysis Program (PRAP) were used to determine material constants. Material constants obtained by the different methods were compared. The results show that the impedance spectroscopy method gives more precise data and in some cases is the "sheet anchor" of correct values for materials with extremely low Q.

References

IEEE Standard on piezoelectricity. ANSI/IEEE Std. 176 - 1987.

M. Alguero, C. Alemany, L. Pardo and A. M. Gonzalez. Method for Obtaining the Full Set of Linear Electric, Mechanical and Electromechanical coefficients and All Related Losses of a Piezoelectric Ceramic. J. Am. Ceram. Soc. 87 (2), 209 (2004).

R. Holland. Representation of dielectric, elastic and piezoelectric losses by complex coefficients. IEEE Trans.Sonics Ultrason. SU-14 (1), 18 (1967).

S. Sherrit, H. D. Wiederick and B.K. Mukherjee. Non-iterative Evaluation of the Real and Imaginary Material Constants of Piezoelectric Resonators. Ferroelectrics 134, 111 (1992).

S. Sherrit, H.D. Wiederick and B.K. Mukherjee. A complete characterization of the piezoelectric, dielectric and elastic properties of Motorola PZT3203HD including losses and dispersion. Medical Imaqinq 1997: Ultrasonic Transducer Engineerinq. SPIE Proceedinqs. 3037, 158 (1997).

S. Sherrit, H. D. Wiederick and B.K. Mukherjee. The Complete Matrix of the Piezoelectric, Dielectric and Elastic Materials Constants of 1-3 Piezoelectric Ceramic/Polymer Composites, Smart Materials. Structures, and Integrated Svstems, SPIE Proceedings, 3241, 327 (1997).

C. Alemany, L. Pardo, B. Jimenez, F. Carmona, J. Mendiola and A.M. Gonzalez. Automatic iterative evaluation of complex material constants in piezoelectric ceramics. J. Phvs. D: Appl. Phys. 27, 148 (1994).

J.G. Smits. Iterative method for accurate determination of the real and imaginary parts of the materials coefficients of piezoelectric ceramics. IEEE Trans. Sonics Ultrason. SU-23 (6), 393-402 (1976).

L.Pardo, C. Alemany, J. Ricote, A. Moure, R. Poyato and M. Alguero.
Iterative methods for the characterization of piezoelectric materials with losses. Proc. Intern. Conf. Material technology and design of integrated piezoelectric devices. Couurmayeur, Italy, 145, 2004.

PRAP (Piezoelectric Resonance Analysis Program). TASI Technical Software Inc. (www.tasitechnical.com).

A.F. Devonshire, Philosphical Magazine Supplement, 3, 85-130, 1954

W.P. Mason, Physical Acoustics and the Properties of Solids (D. Van Nostrand Co. Inc. Princeton 1958).

D.A. Berlincourt, D.R. Curran, H. Faffe, Physical Acoustics I, Part A (W.P. Mason ed., Academic Press 1964).

L.C. Shen, J.A. Kong, Applied Electromagnetism (PWS Engineering, Boston 1983).

C. Alemany, A.M. Gonzalez, L. Pardo, B. Jimenez, F. Carmona and J. Mendiola. Automatic determination of complex constants of piezoelectric lossy materials in the radial mode. J. Phvs. D: Appl.Phvs. 28(5), 945 (1995).